

Vibronic levels of the *EL2* center under uniaxial stress

Liana Martinelli

Dipartimento di Fisica, Università di Pisa, piazza Torricelli 2, 56125 Pisa, Italy

Giuseppe Pastori Parravicini

Dipartimento di Fisica "A. Volta," Università di Pavia, via A. Bassi 6, 27100 Pavia, Italy

(Received 26 December 1991)

We study the vibronic levels of the arsenic antisite defect in GaAs and the optical properties associated with the $A_1 \rightarrow T_2$ transition of the As_{Ga} defect. In our model we include both the Jahn-Teller effect on the T_2 -degenerate states and the effect of a uniaxial stress applied along several crystal directions; the coupled system of electron-vibrational states is handled with the recursion method. With a coupling with a phonon mode of symmetry τ_2 we have calculated the features of the transition line at 8378 cm^{-1} and its replicas; relationships with available experimental data and microscopic models are discussed.

I. INTRODUCTION

The nature and role of the *EL2* defect in controlling the optical and electrical properties of GaAs have been the subjects of a large number of experimental¹⁻¹¹ and theoretical¹²⁻¹⁸ investigations; in effect, this center has acquired a unique position in the semiconductor defect physics both for scientific interest and because of technological importance. In spite of numerous studies, there are still relentless efforts towards unified interpretations of the existing experiments (see, for instance, Ref. 10, in particular Section 11, dedicated to *EL2* and antisite-related defects). Presently, the two most accredited microscopic models in the literature are (i) the isolated antisite defect suggested on the basis of piezospectroscopic studies of optical transitions^{3-7,9,11} and favored by theory to explain the metastable state,¹²⁻¹⁴ (ii) a loosely bound $As_{Ga}-As_i$ complex suggested and corroborated by electron paramagnetic resonance studies⁸ and supported further by optically detected electron nuclear double resonance.^{19,20} Along this line, the contribution of Ref. 21 advances the possibility that the "resonant state" responsible of the 1.039-eV line is a multivalley effect derived from *L* minima. This important possibility is further elaborated in Ref. 17.

In this work we take the isolated antisite model at its face value and explore in depth the consequences of a Jahn-Teller coupling and uniaxial stress. Our purpose is not to add to the wide debate on the microscopic models, but rather to present a workable theoretical approach for the vibronic levels of the *EL2* center. Notice that in the case of the $As_{Ga}-As_i$ pair model, our procedure is in principle still applicable, embodying in the treatment an additional potential with C_{3v} symmetry.

Bearing this in mind, we summarize as follows the principle features of the near-infrared absorption spectrum³ due to the *EL2* defect. The absorption spectrum consists of a photoionization background and an intracenter absorption in the energy region between 1.0 and 1.3 eV with fine structure involving the 1.039-eV (8378 cm^{-1}) line and its replicas³ separated by about 10 meV

(80.6 cm^{-1}). Our interest is focused on this part of the spectrum, and the line at 1.039 eV is referred to as the zero-phonon line (ZPL). The presence of the replicas and the nonlinear behavior with the stress of some of the components in which the $A_1 \rightarrow T_2$ optical transition splits under uniaxial stress support the hint of a dynamical Jahn-Teller effect on the T_2 -degenerate electronic states.³ The coupling of T_2 states with a phonon mode of the same symmetry τ_2 has been investigated by different authors^{15,16} to explain the stress-splitting behavior of the ZPL. Furthermore, a weak Jahn-Teller interaction has been recognized as an important mechanism causing the system to relax into a metastable configuration.²² Incidentally, we notice that a small lattice relaxation is invoked also in the widely studied donor centers known as *DX* centers in $Ga_{1-x}Al_xAs$ alloys,²³ the driving mechanism being a small lattice relaxation linked with the electronic intervalley interference effects.

In this paper we investigate the optical transitions $A_1 \rightarrow T_2$ including on the same footing a linear Jahn-Teller coupling and a linear uniaxial stress (Sec. II); in order to handle the large number of degrees of freedom of our vibronic system, we use the recursion method and the concepts of dipole-carrying states (Sec. III). In Sec. IV we present our results and discuss the intracenter optical-absorption fine structure with piezospectroscopic measurements and microscopic models.

II. THE MODEL HAMILTONIAN

In this section we describe the essential features of our semiempirical model Hamiltonian for a defect in a tetrahedral-symmetry environment. The vibronic system under consideration is constituted by a threefold-degenerate electronic state T_2 in interaction with the lattice vibrations. The lattice models allowed to act on the T_2 electronic level are those having A_1 , E , and T_2 symmetry (but conventionally denoted by α , ϵ , and τ_2 , respectively). The coupling with the total symmetric mode α can produce a shift in the absorption spectrum, but cannot remove degeneracies or explain the replicas observed

experimentally in the spectrum. According to the literature,^{15,16} it is expected that the coupling with the interaction mode ϵ is negligible; we also agree, and corroborate this point by showing, with the recursion method, that the $T_2 \otimes \epsilon$ coupling does not provide the replicas. Thus we are left with the only significative modes of symmetry τ_2 .

Let us indicate with Ψ_x , Ψ_y , and Ψ_z the degenerate electronic states of symmetry T_2 for the nuclei fixed in the symmetry position. Following the literature,²⁴ we adopt a cluster model for the lattice vibrations, and we consider a linear coupling with an effective vibrational mode of symmetry τ_2 . By expanding the interaction energy up to the second order in the normal symmetrized coordinates Q_x , Q_y , and Q_z and fully exploiting the tetrahedral symmetry of the vibronic system, we obtain the following $T_2 \otimes \tau_2$ Hamiltonian:

$$H = E_e - \frac{\hbar^2}{2M} \left[\frac{\partial^2}{\partial Q_x^2} + \frac{\partial^2}{\partial Q_y^2} + \frac{\partial^2}{\partial Q_z^2} \right] + V_T \begin{pmatrix} 0 & Q_z & Q_y \\ Q_z & 0 & Q_x \\ Q_y & Q_x & 0 \end{pmatrix} + \frac{1}{2} M \omega^2 (Q_x^2 + Q_y^2 + Q_z^2). \quad (1)$$

In Eq. (1), E_e is the energy of the degenerate electron state, V_T is the linear coupling constant with the vibrational mode τ_2 , and ω is the angular frequency of the mode; the quantities in Eq. (1) that are not written explicitly in the matrix form are intended to be multiplied by the identity 3×3 unit matrix. This is a well-known Jahn-Teller Hamiltonian studied by a numbers of authors starting from the pioneer works of Ham²⁵ and Caner and Englman and Englman, Caner, and Toaff.²⁶ For more recent treatments, see, for example, the book of Perlin and Wagner.²⁷

Let us consider now the effect on the uniaxial stress on the electron of the isolated As_{Ga} . This effect can be described, to the lower order, by a deformation Hamiltonian with terms linear in the stress tensor components (see, for instance, Refs. 15 and 28). In the following we need the explicit form of the stress interaction on the basis of the T_2 electron states for the different directions along which the uniaxial stress can be applied. For the stress parallel to the [001], [110], and [111] directions, we have, respectively,

$$\begin{pmatrix} \Delta + a's & ds_{yz} & ds_{zx} & ds_{xy} \\ ds_{yz} & as + \frac{b}{2}(\sqrt{3}s_\epsilon - s_\theta) & cs_{xy} & cs_{zx} \\ ds_{zx} & cs_{xy} & as - \frac{b}{2}(\sqrt{3}s_\epsilon + s_\theta) & cs_{yz} \\ ds_{xy} & cs_{zx} & cs_{yz} & as + bs_\theta \end{pmatrix}. \quad (3)$$

In the fourfold-excited manifold of Davies, the energy separation Δ between the A_1 and the T_2 states is taken as a disposable parameter, which must be determined from the experimental piezospectroscopic data; then the effect

$$V_{st}[001] = s \begin{pmatrix} a-b & 0 & 0 \\ 0 & a-b & 0 \\ 0 & 0 & a+2b \end{pmatrix}, \quad (2a)$$

$$V_{st}[110] = s \begin{pmatrix} a + \frac{b}{2} & \frac{c}{2} & 0 \\ \frac{c}{2} & a + \frac{b}{2} & 0 \\ 0 & 0 & a-b \end{pmatrix}, \quad (2b)$$

$$V_{st}[111] = s \begin{pmatrix} a & \frac{c}{3} & \frac{c}{3} \\ \frac{c}{3} & a & \frac{c}{3} \\ \frac{c}{3} & \frac{c}{3} & a \end{pmatrix}. \quad (2c)$$

Here the parameters a , b , and c are phenomenological constants related to the stress splitting of an isolated As_{Ga} , and s is the magnitude of the stress.

In Table I, we report for convenience the splitting of the T_2 state under the effect of a uniaxial stress along the [001], [110], and [111] directions, respectively. Because of the reduction of the symmetry from T_d to D_{2d} ([001] stress), C_{2v} ([110] stress), and C_{3v} ([111] stress) symmetry, we expect that the $A_1 \rightarrow T_2$ optical transition is split into two, three, and two lines, respectively.

It is evident that all the splittings of Table I are linear in s , while the experiments^{3,6} show nonlinear effects, in particular for the transitions from the A_1 ground state to the A_1 symmetry sublevel; this fact, together with the replicas in the case without stress, are indications of a Jahn-Teller coupling active on the T_2 level. In the literature, the calculations until now available treat separately the problem of the stress and the problem of the Jahn-Teller interaction. In the work of Davies,¹⁶ for instance, the complicated Jahn-Teller system is replaced by a fourfold-excited manifold, namely the excited T_2 state and an A_1 level, whose occurrence and origin is well established in works on vibronic systems.^{25,26} Under stress, the perturbation on the excited A_1 and T_2 states leads to the Hamiltonian of type:¹⁶

of a weak Jahn-Teller coupling is inferred.

In the present work, by treating on the same footing the Jahn-Teller coupling and the stress Hamiltonian, we generalize and improve the point of view of Ref. 16, and

TABLE I. Effect of the uniaxial stress, along the [001], [110], and [111] directions on the T_2 level. The expressions of the shift of the corresponding sublevels are given.

Stress axis	Label	Expression
[001]	E	$(a+2b)s$
	B_2	$(a-b)s$
[110]	B_2	$[a+(b-c)/2]s$
	A_1	$(a-b/2- b /2)s$
	B_1	$[a+(b+c)/2]s$
[111]	E	$(a-c/3)s$
	A_1	$(a+c/3- c /3)s$

we can find the replica and calculate the oscillator strength. This conceptual advantage is achieved at the expense of increased complexity of the vibronic systems under consideration, which now contain a large number of degrees of freedom; these large systems, however, have matrix Hamiltonians of sparse form that can be conveniently handled with the iterative technique of the recursion method. Incidentally, we notice that the Hamiltonian of Eq. (3) is also formally obtained in the work of Lannoo, Delerue, and Allan¹⁷ from many-valley interference effects; although we do not discuss these models, we notice that lattice relaxation could be accounted for with procedures similar to those presented in this work.

III. RECURSION METHOD AND OPTICAL TRANSITIONS

The recursion method^{29,30} has been shown to be a very effective tool to treat Jahn-Teller systems³¹⁻³³ even in the

case of strong coupling. Here we briefly summarize some technical aspects for vibronic systems, including Jahn-Teller distortion and uniaxial stress. Let us consider the Hamiltonian of Eq. (1), supplemented with the uniaxial stress contributions of Eqs. (2). It is convenient to introduce the phonon creation and annihilation operators a_x^\dagger, a_x ; a_y^\dagger, a_y and a_z^\dagger, a_z for the partners of the mode of symmetry τ_2 ; the corresponding states can be labeled by the occupation numbers l, m , and n , respectively. The basis functions chosen are thus the direct product $|\Psi_i; lmn\rangle$ of the degenerate electron functions $|\Psi_i\rangle$ ($i=x, y, z$) and of the vibrational states $|lmn\rangle$.

The total Hamiltonian describing the system of interest is the sum of the electronic part (H_e), the vibrational part (H_L), and the electron-lattice coupling part (H_{e-L}), and the stress part (H_{st}) and can be written as

$$H = H_e + H_L + H_{e-L} + H_{st} . \quad (4)$$

We take the energy of the electron state as the reference energy. On the basis functions $|\Psi_i; lmn\rangle$, H_L can be written as

$$H_L = \hbar\omega \sum_{\substack{i=x,y,z \\ l,m,n=0,\infty}} (l+m+n+\frac{3}{2}) |\Psi_i; lmn\rangle \langle \Psi_i; lmn| , \quad (5)$$

where $\hbar\omega$ is the energy of the mode τ_2 . The electron-lattice interaction becomes

$$H_{e-L} = k_T \hbar\omega \sum_{l,m,n=0,\infty} (|\Psi_x; lmn\rangle \langle \Psi_y; lmn| + |\Psi_y; lmn\rangle \langle \Psi_x; lmn|) (a_z + a_z^\dagger) + \text{cyclic interchange of } x, y, z \text{ indices} , \quad (6)$$

where the adimensional coupling constant k_T is $2V_T / [\sqrt{3}(2M\hbar)^{1/2}\omega^{3/2}]$. The stress Hamiltonian H_{st} assumes different expressions with the direction of uniaxial stress [see Eqs. (2)]. We give explicitly, as an example, the expression of H_{st} [001]:

$$H_{st}[001] = \sum_{l,m,n=0,\infty} |\Psi_x; lmn\rangle (a-b)s \langle \Psi_x; lmn| + |\Psi_y; lmn\rangle (a-b)s \langle \Psi_y; lmn| + |\Psi_z; lmn\rangle (a+2b)s \langle \Psi_z; lmn| . \quad (7)$$

We can now apply the general concepts and methodology of the recursion method, and the initial and large sparse matrix can be transformed into a manageable tridiagonal one, whose dimension is the number of iterations performed. If we take as the initial state of the recursion the dipole-carrying state,¹³ we can conveniently describe the absorption spectrum and the relative intensity of the lines upon diagonalization of the tridiagonal matrix.

IV. RESULTS AND DISCUSSION

First of all, we wish to consider more closely the approximation of neglecting the vibrational mode of ε symmetry. The system $T_2 \otimes \varepsilon$ treated by means of the recursion technique allows us to obtain analytic expression for a_ν and b_ν (diagonal and off-diagonal parameters of the semi-infinite linear chain); choosing as the initial state a

zero-phonon vibronic state and taking the T_2 level as the reference energy, we obtain

$$a_\nu = (\nu+1)\hbar\omega , \quad \nu=0, 1, \dots , \quad (8)$$

$$b_\nu^2 = \nu V_T^2 , \quad \nu=1, 2, \dots .$$

After diagonalizing the seminfinite chain with parameters given by the Eq. (8), we arrive at a Poissonian shape of the absorption; thus we conclude that the $T_2 \otimes \varepsilon$ coupling could not explain the experimental optical absorption, where a ZPL is followed by several replicas. In this way, alternative to what is already accepted in the literature, we can confirm the Baraff conclusions¹⁵ excluding, in this region of the absorption spectrum, a significative coupling with a mode of symmetry ε .

In the case of the $T_2 \otimes \tau_2$ vibronic model, the coefficients a_ν and b_ν are not analytic and must be calcu-

lated numerically with recursions (or over-recursions). A suitable choice of the initial state allows us to evaluate the energy and the intensity of the T_2 level, the A_1 excited level, and the seven sublevels in which the T_2 state is split by uniaxial stress.

We can now examine that part of the optical-absorption spectrum of the *EL2* defect which consists of the ZPL at 8378 cm^{-1} and his replicas. We consider first the situation without uniaxial stress in order to settle the parameters for the Jahn-Teller effect. Because the energy separation of the replicas in the absorption spectrum is very close to the transverse-acoustic-phonon energy ($\hbar\omega = 80.6\text{ cm}^{-1}$) at the boundary of the Brillouin zone, we choose this value for the phonon-mode energy. We now have to consider some reasonable criterion for the selection of the Jahn-Teller energy E_{JT} . For this purpose, we notice that when the Jahn-Teller energy is varied, or alternatively the Huang-Rhys factor S (defined by means of the relation $E_{JT} = S\hbar\omega$) is varied, the absorption shape exhibits quite different features. For $S \ll 1$ we obtain a very intense ZPL and no replicas appear. Increasing S , the oscillator strength is gradually transferred to levels separated from the first and between them by about $\hbar\omega$. For $S = 1 \pm 0.4$ (or $k_T = 1 \pm 0.2$) we obtain a ZPL followed by four replicas of comparable intensity separated by about $\hbar\omega$. For larger S , the ZPL tends to disappear. Notice that the values for S which give the replicas are in agreement with those proposed by Davies.¹⁶ In most of the following calculations, we used $S = 1$ as a typical value of the Huang-Rhys factor for our problem. From a computational point of view, a cluster of eight phonons and about 30 over-recursions was sufficient to give the ZPL and the lowest replica with reasonable accuracy. The initial state was the dipole-carrying state $f_0 = |\psi_i, 000\rangle$.

In order to obtain the vibronic levels of symmetry A_1 , we have applied the recursion procedure, taking as the initial state, for instance, the vibronic one-phonon state at symmetry $A_1: f_0 = [|\psi_x; 100\rangle + |\psi_y; 010\rangle + |\psi_z; 001\rangle] / \sqrt{3}$; in this way we can find the energy of the A_1 excited states. Let us indicate by Δ the energy difference between the excited state of symmetry A_1 and the ground state of symmetry T_2 . The shift Δ changes with the Huang-Rhys factor; the behavior is shown in Fig. 1, and looks like a decreasing exponential with S , as also previously predicted,¹⁵ but in a different way. For our suggested values of S , the energy difference Δ is in the range of $19.9\text{--}38.5\text{ cm}^{-1}$; for $S = 1$ we have $\Delta = 28\text{ cm}^{-1}$. Thus our model agrees, also quantitatively, with the assumption made by Davies¹⁶ of an A_1 level higher than the T_2 state.

After the reasonably satisfactory analysis in the absence of uniaxial stress, we now consider the simultaneous introduction of the Jahn-Teller and stress Hamiltonian terms. Different coefficients of the recursion relations for the different direction of the stress and initial states of appropriate symmetry are needed. The constants a , b , and c are taken equal to 0.10 , 0.056 , and $-1.0\text{ cm}^{-1}\text{ MPa}^{-1}$, respectively, in such a way to reproduce the experimental measurements.^{1,6}

For the stress in the $[001]$ direction, the sublevels E

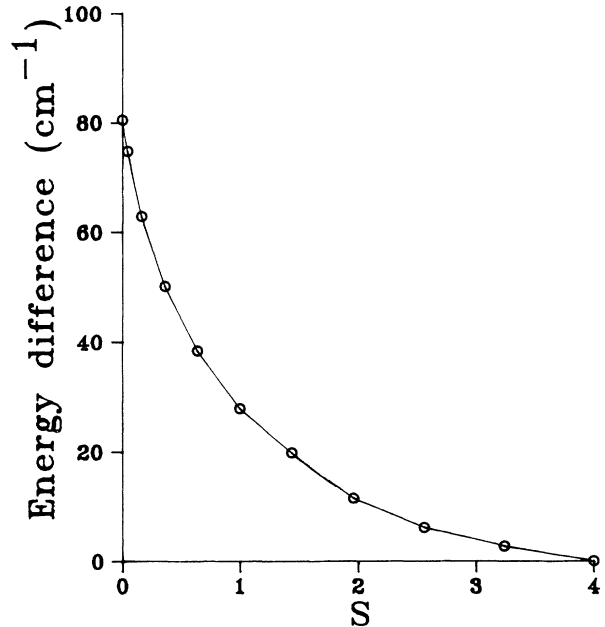


FIG. 1. Energy difference Δ between the vibronic A_1 level and the T_2 levels vs the Huang-Rhys factor S . The energies are in cm^{-1} . The energy of the coupling mode is $\hbar\omega = 80.6\text{ cm}^{-1}$.

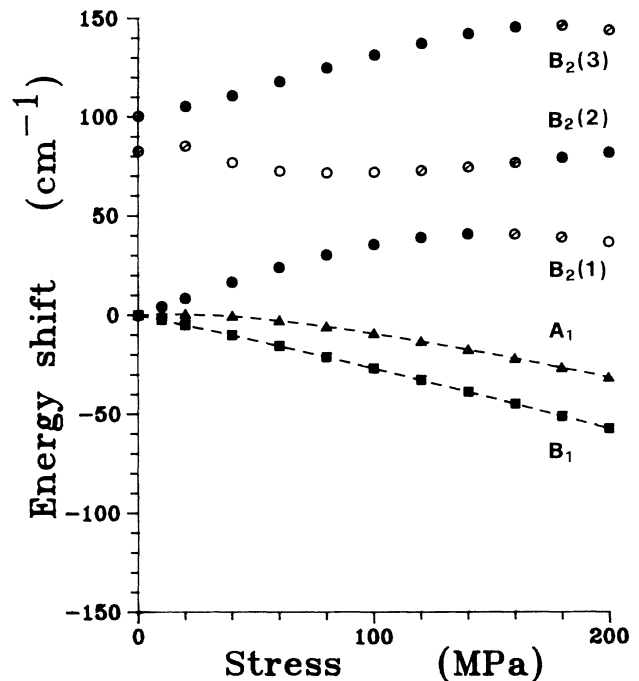


FIG. 2. Energy in cm^{-1} of the B_1 , A_1 , $B_2(1)$, $B_2(2)$, and $B_2(3)$ sublevels (labeled, respectively, by \blacksquare , \blacktriangle and \circ) as a function of the stress in the $[110]$ direction. The magnitude of the stress is in MPa. The parameters used are $\hbar\omega = 80.6\text{ cm}^{-1}$, $S = 1$, $a = 0.10$, $b = 0.056$, and $c = -1.0\text{ cm}^{-1}\text{ MPa}^{-1}$. As a guide to the eye, for what concerns relative intensities I , the symbols \circ , \oplus , \oplus , and \bullet denote relative intensities in the range $[I < 0.05]$, $[0.05 \leq I < 0.10]$, $[0.10 \leq I < 0.15]$, and $[I \geq 0.15]$, respectively.

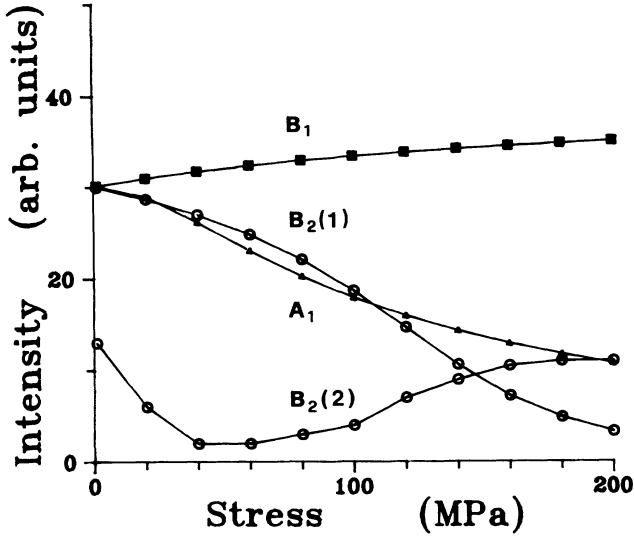


FIG. 3. Intensity (in arbitrary units) of the B_1 , A_1 , and $B_2(1)$, and $B_2(2)$ sublevels (labeled, respectively, by \blacksquare , \blacktriangle , \circ) for the stress in the [110] direction as a function of the stress.

and B_2 are obtained with the initial state $f_0^{(E)} = |\psi_x; 000\rangle$ (or the partner $|\psi_y; 000\rangle$) and $f_0^{(B_2)} = |\psi_z; 000\rangle$, respectively. The sublevels E and B_2 depend linearly on the stress, and the magnitude of the splitting for unit stress between them is found to be $0.035 \text{ cm}^{-1} \text{ MPa}^{-1}$, in good agreement with the experimental value⁶ of $0.036 \text{ cm}^{-1} \text{ MPa}^{-1}$.

For the stress in the [110] direction, the initial states reproducing the B_2 , A_1 , and B_1 sublevels are $f_0^{(B_2)} = [|\psi_x; 000\rangle - |\psi_y; 000\rangle]/\sqrt{3}$, $f_0^{(A_1)} = |\psi_z; 000\rangle$, and $f_0^{(B_1)} = [|\psi_x; 000\rangle + |\psi_y; 000\rangle]/\sqrt{2}$, respectively. The energy levels as a function of the applied uniaxial stress are shown in Fig. 2. The sublevel B_1 moves linearly with the magnitude of the stress s and maintains this intensity almost constantly. The A_1 sublevel shows clearly a nonlinear behavior and the intensity decreases of about 30% for stress of $\approx 200 \text{ MPa}$, as found experimentally. More complicated and more interesting is the behavior of the sublevel B_2 . In Fig. 2 we have reported the ground B_2 sublevel and the lowest excited one [denoted, respectively, $B_2(1)$, $B_2(2)$, and $B_2(3)$]. For stress up to $\approx 100 \text{ MPa}$, the $B_2(1)$ state moves linearly and has intensity higher than $B_2(2)$. For larger stress, the intensity of $B_2(1)$ decreases and that of $B_2(2)$ increases. In Fig. 3 we give the calculated intensity of the sublevels A_1 , B_1 , $B_2(1)$, and $B_2(2)$ versus the magnitude of the stress. We think that at large s , say $s > 140 \text{ MPa}$, the experiments reveal the $B_2(2)$ level. On the other hand, in Ref. 5 there are not experimental data for $110 < s < 200 \text{ MPa}$, and in Ref. 3 there is some uncertainty at about 120 MPa . Thus the presently available experimental data are too fragmentary to definitely confirm the behavior of $B_2(1)$ and $B_2(2)$, but nevertheless are compatible with the exchange of the intensity between $B_2(1)$ and $B_2(2)$ levels put in light by our calculations. Finally, for what concerns the intensity of A_1 and B_1 sublevels, because of this small

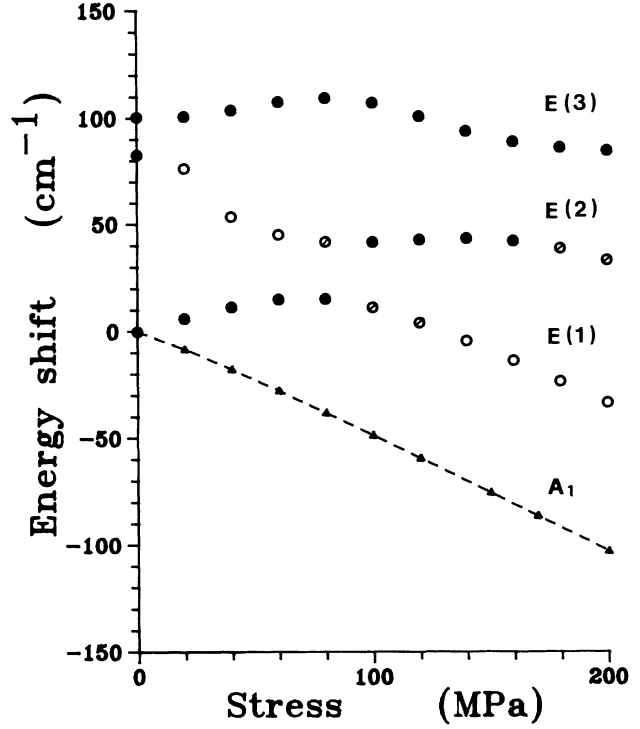


FIG. 4. Energy (in cm^{-1}) of the A_1 and E sublevels (labeled, respectively, by \blacktriangle and \circ) as a function of the stress in the [111] direction. The parameters used are the same as in Fig. 2.

dependence, we can certainly say that the agreement with our calculations is satisfactory.

We consider now the stress in the [111] direction. The initial states reproducing the E and A_1 sublevels are $f_0^{(E)} = [|\psi_x; 000\rangle + |\psi_y; 000\rangle - 2|\psi_z; 000\rangle]/\sqrt{6}$ or the partner $f_0^{(E)} = [|\psi_x; 000\rangle - |\psi_y; 000\rangle]/\sqrt{2}$; and $f_0^{(A_1)} = [|\psi_x; 000\rangle + |\psi_y; 000\rangle + |\psi_z; 000\rangle]/\sqrt{3}$. The results for the [111] direction are reported in Fig. 4. The behavior of the A_1 sublevel is slightly nonlinear and it agrees very well with the experimental data. The lowest E sublevel presents some similarities with the B_2 [110] sublevel: at the beginning it is almost linear with the stress, but with decreasing intensity. Separated by about one $\hbar\omega$, other vibronic levels appear, with interference effects apparent on the relative intensity. For s greater than 80 MPa , the second E level, $E(2)$, becomes important; for greater s ($s > 140 \text{ MPa}$), the third E level predominates; at 200 MPa a reasonable agreement with the experimental shift is obtained by making a weighted average with the intensity between the $E(2)$ and $E(3)$ levels.

We wish to notice that our model, together with the recursion method, allows us to also obtain the features of the replicas under uniaxial stress, and it would be interesting to compare our data with more systematic experimental data. Until now the only measurements (known to us) on the effect of uniaxial stress on replicas are related to the photoluminescence spectra⁹ centered at 0.61 eV , due to the transitions from a shallow excited state of neutral *EL2* to the deep *EL2* ground state.

The presently available piezoabsorption optical experiments and our theoretical results seem to indicate that the four-fold excited manifold of Davies¹⁶ (this manifold is a synopsis of the complete Jahn-Teller system studied in the present paper) contains some basic features of the center and entails moderate lattice relaxation. However, it could be premature to be conclusive on the underlying microscopic model of the *EL2* center. Notice, in fact, that the Hamiltonian that describes double donors associated with the interfering *L* valleys¹⁷ leads qualitatively to a resonant four-fold excited manifold; localization effects and oscillator strength in the presence of lattice relaxa-

tion and breaking of tetrahedral symmetry should be analyzed comparatively. Experimental piezospectroscopic data concerning replicas under uniaxial stress would be desirable for a better comprehension of the microscopic structure of this challenging defect.

ACKNOWLEDGMENTS

This work was supported by Gruppo Nazionale Struttura della Materia and Consorzio Interuniversitario Nazionale Fisica della Materia.

- ¹For a review see M. Kaminska, in *Proceedings of the 7th General Conference of the Condensed Matter Division of the European Physical Society*, edited by F. Bassani, G. Grosso, G. Pastori Parravicini, and M. P. Tosi [Phys. Scr. **T19**, 551 (1987)].
- ²G. M. Martin, Appl. Phys. Lett. **39**, 747 (1981).
- ³M. Kaminska, M. Skowronski, J. M. Parsey, and H. G. Gatos, Appl. Phys. Lett. **43**, 302 (1983); see also M. Kaminska, M. Skowronski, and W. Kuszko, Phys. Rev. Lett. **55**, 2204 (1985).
- ⁴M. Skowronski, J. Lagowski, and H. C. Gatos, Phys. Rev. B **32**, 4264 (1985).
- ⁵M. Hoinkis, E. R. Weber, W. Walukiewicz, J. Lagowski, M. Matsui, H. C. Gatos, B. K. Meyer, and J. M. Spaeth, Phys. Rev. B **39**, 5538 (1989).
- ⁶P. Trautman, J. P. Walczak, and J. M. Baranowski, Phys. Rev. B **41**, 3074 (1990).
- ⁷M. Baj, P. Dreszer, and A. Babinski, Phys. Rev. B **43**, 2070 (1991).
- ⁸H. J. von Bardeleben, D. Stievenard, J. C. Bourgoin, and A. Huber, Appl. Phys. Lett. **47**, 970 (1985); H. J. von Bardeleben, D. Stievenard, D. Deresmes, A. Huber, and J. C. Bourgoin, Phys. Rev. B **34**, 7192 (1986).
- ⁹M. K. Nissen, A. Villemaire, and M. L. W. Thewalt, Phys. Rev. Lett. **67**, 112 (1991); in *Proceedings of the Sixteenth International Conference on Defects in Semiconductors, Lehigh University, Pennsylvania, 1991*, edited by G. Davies, G. G. DeLeo, and M. Stavola (Trans Tech, Zürich, 1992), p. 893.
- ¹⁰For other recent papers, see, for instance, *Proceedings of the Sixteenth International Conference on Defects in Semiconductors, Lehigh University, Pennsylvania, 1991* (Ref. 9), Sec. 11.
- ¹¹G. A. Samara, D. W. Vook, and J. F. Gibbons, Phys. Rev. Lett. **10**, 1582 (1992).
- ¹²J. Dabrowski and M. Scheffler, Phys. Rev. Lett. **60**, 2183 (1988); Phys. Rev. B **40**, 10391 (1989); in *Proceedings of the Sixteenth International Conference on Defects in Semiconductors, Lehigh University, Pennsylvania, 1991* (Ref. 9), p. 735.
- ¹³D. J. Chadi and K. J. Chang, Phys. Rev. Lett. **60**, 2187 (1988).
- ¹⁴M. J. Caldas, J. Dabrowski, A. Fazzio, and M. Scheffler, Phys. Rev. Lett. **65**, 2046 (1990).
- ¹⁵G. A. Baraff, Phys. Rev. B **40**, 1030 (1989); **41**, 9850 (1990).
- ¹⁶G. Davies, Phys. Rev. B **41**, 12303 (1990).
- ¹⁷M. Lannoo, C. Delerue, and G. Allan, in *Proceedings of the Sixteenth International Conference on Defects in Semiconductors, Lehigh University, Pennsylvania, 1991* (Ref. 9), p. 865.
- ¹⁸G. A. Baraff and M. A. Schlüter, Phys. Rev. B **45**, 8300 (1992).
- ¹⁹D. M. Hofmann, B. K. Meyer, F. Lohse, and J. M. Spaeth, Phys. Rev. B **13**, 1187 (1984).
- ²⁰B. K. Meyer, D. M. Hofmann, J. R. Niklas, and J. M. Spaeth, Phys. Rev. B **36**, 1332 (1987).
- ²¹H. J. von Bardeleben, Phys. Rev. B **40**, 12546 (1989).
- ²²G. B. Bachelet and M. Scheffler, in *Proceedings of the Seventeenth International Conference on the Physics of Semiconductors*, edited by D. J. Chadi and W. A. Harrison (Springer-Verlag, New York, 1985), p. 755.
- ²³J. C. Bourgoin and H. J. von Bardeleben, Phys. Rev. B **40**, 10006 (1989); M. Zazoui, S. L. Feng, and J. C. Bourgoin, *ibid.* **41**, 8485 (1990); G. Pastori Parravicini, L. Resca, R. D. Graft, and D. J. Lohrmann, Solid State Commun. **78**, 655 (1991).
- ²⁴M. D. Sturge, in *Solid State Physics*, edited by F. Seitz, D. Turnbull, and H. Ehrenreich (Academic, New York, 1967), Vol. 20, p. 92.
- ²⁵F. S. Ham, Phys. Rev. **138**, A1727 (1965).
- ²⁶M. Caner and R. Englman, J. Chem. Phys. **44**, 4054 (1966); R. Englman, M. Caner, and S. Toaff, J. Phys. Soc. Jpn. **29**, 306 (1970); see also R. Englman, *The Jahn-Teller Effect in Molecules and Crystals* (Wiley, New York, 1972).
- ²⁷*The Dynamical Jahn-Teller Effect in the Localized Systems*, edited by Yu. E. Perlin and M. Wagner (North-Holland, Amsterdam, 1984).
- ²⁸A. K. Ramdas and S. Rodriguez, in *Progress in Electron Properties of Solids*, edited by E. Doni, R. Girlanda, G. Pastori Parravicini, and A. Quattropani (Kluwer, Dordrecht, 1989), p. 65.
- ²⁹R. Haydock, V. Heine, and M. J. Kelly, J. Phys. C **5**, 2845 (1972); **8**, 2591 (1975); see also D. W. Bullet, R. Haydock, V. Heine, and M. J. Kelly, in *Solid State Physics*, edited by H. Ehrenreich, F. Seitz, and D. Turnbull (Academic, New York, 1980), Vol. 35.
- ³⁰See, for instance, G. Grosso and G. Pastori Parravicini, Adv. Chem. Phys. **62**, 81 (1985); **62**, 133 (1985), and references quoted therein.
- ³¹L. Martinelli, M. Passaro, and G. Pastori Parravicini, Phys. Rev. B **39**, 13343 (1989); **43**, 8395 (1991).
- ³²M. C. M. O'Brien and S. N. Evangelou, J. Phys. C **13**, 611 (1980); Solid State Commun. **36**, 29 (1980); M. C. M. O'Brien, J. Phys. C **16**, 85 (1983); **16**, 6345 (1983); **18**, 4963 (1985).
- ³³S. Muramatsu and N. Sakamoto, J. Phys. Soc. Jpn. **44**, 1640 (1978); **46**, 1273 (1979); Phys. Rev. B **17**, 868 (1978).